A quick-retrieval high-speed digital framing camera

A. H. Sato, J. Yee, and P. M. Bellan
California Institute of Technology, Pasadena, California 91125

(Received 22 April 1993; accepted for publication 26 August 1993)

A new high-speed digital framing camera is described. The design is built around a rotating polygon mirror that provides a framing rate of 24 000 frames/s. The camera electronics digitizes an image into a 32×104 grid of pixels, where the second dimension of the grid can be varied and is determined by the 8 bit computer-aided measurement and control digitizer sampling rate. Available digitizer memory provides for 314 frames at this horizontal resolution. The advantages over other available high-speed framing cameras are (1) low cost of the system provided the digitizers are available, (2) rapid retrieval of a recorded event, and (3) the ease with which the system can be used. Sample results from an application in high-power arc photography are given to illustrate the system's spatial and temporal resolution.

I. INTRODUCTION

High-speed photography has long been used to record images of self-luminous objects such as arcs and explosions. Moving picture cameras, capable of framing rates of $\sim10^3$ to a few times 10^4 frames/s, have evolved since the 1920's, and optoelectronic shutters and image converter cameras have extended framing rates to as high as 10^7 frames/s.[1] Framing rates of $\sim10^3$ to $\sim10^4$ frames/s have proven useful in studying various types of arc discharge such at circuit breaker arcs,[2] arc spots on cathodes,[3] and high-power arcs.[4,5] High-speed photography has been crucial in a recent arc stabilization experiment for observing various arc stability regimes of a model furnace arc.[6] These latter experiments also demonstrated three shortcomings associated with conventional fast framing cameras: (1) complexity, (2) high cost, and (3) substantial delay before the movie can be viewed (e.g., film developing, rewinding, etc.). These difficulties were overcome by a low resolution digital computer-aided measurement and control (CAMAC) based framing camera introduced in Ref. 6 that allowed for immediate retrieval of a movie after the event had been recorded.

This article describes a higher resolution version[7] of this CAMAC based camera which maintains the rapid retrieval feature, the ease of camera operation, and the relatively low cost of the system (beyond the investment in CAMAC digitizing modules). The spatial resolution of the system has been increased by a factor of ~10, at the cost of only a factor of ~2 in the framing rate. Section II of this article describes the improved camera design, Sec. III presents sample excerpts from movies of an unstable arc, and Sec. IV presents a discussion of the camera's capabilities.

II. THE CAMERA DESIGN

A. Overview

Figure 1 shows a top view of the camera and the arc (object plane) being photographed; directions in the plane of the drawing will be referred to as "horizontal," and directions normal to the plane of the drawing will be referred to as "vertical." A ray of light from the object plane (the arc) passes through an aperture A, reflects off of a facet of the rotating mirror RM, passes through lens L1 and L2, and is focused in the image plane where a detector is located. The axis of rotation of the polygon mirror is perpendicular to the plane of the drawing, and the detector is a linear array of 32 photodiodes extending along the same vertical direction. The focal length and position of lens L1 is chosen to form a real image before lens L2; the horizontal orientation of the image is indicated by the arrow symbols. As the mirror RM rotates, the image is scanned in the horizontal direction, perpendicular to the linear diode array detector. For example, if the mirror rotates in the counterclockwise direction, the tail of the arrow reaches the detector first, followed by the head of the arrow. As the image moves across the detector, each photodiode of the array samples a horizontal band in the image. The signal is then digitized by a transient digitizer, one channel per photodiode. The data stored in the memory of the transient digitizers is then reassembled to form images or frames, and finally the frames are consecutively displayed on a video monitor to form moving picture images.

B. Optics

The spacing and dimensions of the optical components are listed in Table I. This section discusses the selection of these particular values.

We first discuss the role of the aperture A. The aperture is required because of the multiple mirrors (i.e., facets) constituting the rotating mirror RM. The rotating mirror (Lincoln Laser Co., model DT-48-282-025) is an aluminum polygon of 48 sides, each facet being a 0.45 cm wide$\times$0.65 cm high polished mirror. Roughly a quarter of these facets are capable of reflecting rays of light from the object plane toward lens L1. Since the facets make an angle $\theta_0\equiv360°/48=7.5°$ with respect to one another, the image seen through one facet is displaced by an angle $2\theta_0$ from the image seen through an adjacent facet. (The factor of 2 arises from the law of reflection for light rays incident on a facet). If the aperture A were not present, images reflected from adjacent facets would overlap. However, if an aperture restricts the field of view to a full angular width of $2\theta_0$ or less, the images from adjacent facets are too small to

 0034-6748/93/64(12)/3542/6/$6.00

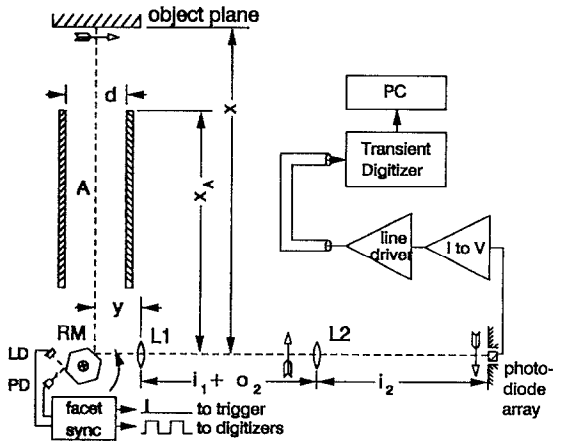

FIG. 1. Top-view schematic of the rotating mirror camera showing the optical components, one of the 32 photodiode channels, and the facet sync circuit. A: aperture; RM: polygon rotating mirror; L1, L2: lenses, LD: laserdiode; PD: photodiode. The spacing between optical components—x, x_A, y, i_1+o_2, and i_3—are given in Table I. The facet sync circuit's "to trigger" signal begins the digitizers' sampling at the same point in the rotation of a facet. The "to digitizer" signal is measured by a digitizer to find the frame period. Current-to-voltage converters and line drivers are used to feed the photodiode signal to the transient digitizers. The drawing for the mirror is simplified; the polygon actually has 48 sides.

overlap. Our experiment uses a tube of diameter $d=11.1$ cm with one end at a distance $x_A \approx 46$ cm from the facet, such that $\tan\theta_0 > d/(2x_A)$. In this case, the visible field of view has a half angle of 6.9°.

The choice of lens L1 is determined by the total vertical magnification M_{tot} desired and the object distance o_1 for lens L1. Our experiment requires a magnification of 2.3, and $o_1 \equiv x+y$ is determined by other construction constraints. Taking these as independent variables, lens L1 was chosen to minimize the distance from L1 to the detector. This distance F may be expressed as

$$F(M_1,f_2) \equiv i_1+o_2+i_2 = -M_1 o_1 + (1-M_{\text{tot}}/M_1)(1-M_1/M_{\text{tot}})f_2, \quad (1)$$

where $M_1 = -i_1/o_1$ is the magnification of lens L1 and f_2 is the focal length of lens L2. With f_2 fixed, a minimum in $F(M_1,f_2)$ occurs at

$$M_1 = -M_{\text{tot}}/(1+M_{\text{tot}}o_1/f_2)^{1/2}. \quad (2)$$

TABLE I. Parameters for the optical system in Fig. 1.

Item	Dimension or spacing (cm)
x	62
x_A	46
d, aperture diameter	11
y	8.5
i_1+o_2	33
i_2	32
f_1, focal length of lens L1	20
f_2, focal length of lens L2	4.6

However at fixed M_1 (where $M_1<0$), $F(M_1,f_2)$ is monotonically increasing with f_2. It is therefore advantageous to choose f_2 as small as possible. Since we preferred to use 5 cm diam lenses, f_2 was limited by the available 5 cm diam lenses, and a lens of $f_2 \sim 4.6$ cm was selected. M_1 and M_2 are thus determined, and the focal length f_1 for lens L1, the image distances i_1 and i_2, and object distance o_2 can be estimated by thin lens formulas

$$f_1 = o_1/(1-1/M_1), \quad i_1 = M_1 o_1, \quad o_2 = f_2(1-1/M_2), \quad i_2 = f_2(1-M_2). \quad (3)$$

C. The rotating mirror

The rotating mirror spins at 30 000 rpm with a period that is stable to 0.015%. This gives a framing rate of 24 000 frames/s, or 41.7 μs per frame. By examining the behavior of the virtual image formed by a mirror facet, it can be shown that the image travels across the photodiode detector at a constant speed, to a good approximation, when $\theta_0 \ll 1$ and $(R\theta_0)/x \ll 1$, where θ_0 is the angle between facet normals, R is the mean radius of the polygon mirror, and x is the distance between the object plane and the facet which is casting an image on the detector. The first condition states that the polygon angle is small, implying a many-sided polygon mirror. The second condition further requires that the width of a facet is small compared to the distance between the facet and object plane. Both of these conditions are satisfied in our experiment, hence the assumption of linear image motion holds.

D. Trigger synchronization

The framing rate is monitored by measuring the modulation of a light beam reflected from the turning facets. (See Figure 1.) A port in the mirror housing permits a view of the facets. A LN9705P laser diode positioned at one side of the port emits a steady beam toward a facet, while a PN334 PIN photodiode stationed at the other edge of the port receives the modulated light.

The signal from the photodiode is fed to a comparator to generate a rectangular wave form that is synchronous with the appearance of images at the photodiode detector array. This signal is measured by the transient digitizers once (for a given digitizer sampling rate) to determine the mean number of samples that defines a frame. This number is used when later retrieving image data from the digitizers' memory to properly retrieve complete frames. There may be a phase shift between the leading edge of an image at the detector and the synchronizing rectangular wave form, but a temporal offset can easily be added to center the images within a frame during display.

The electrical schematic for the facet detector circuit is shown in Fig. 2. The laser diode and the PIN photodiode appear in the upper part of the schematic. The lower part of the schematic shows the trigger source for the transient digitizers. The "trigger in" input to the left 74LS74 flip-flop comes from a manually generated trigger initiating the rest of the experiment. The right flip-flop is enabled only after the left flip-flop has been set, and the output pulse of

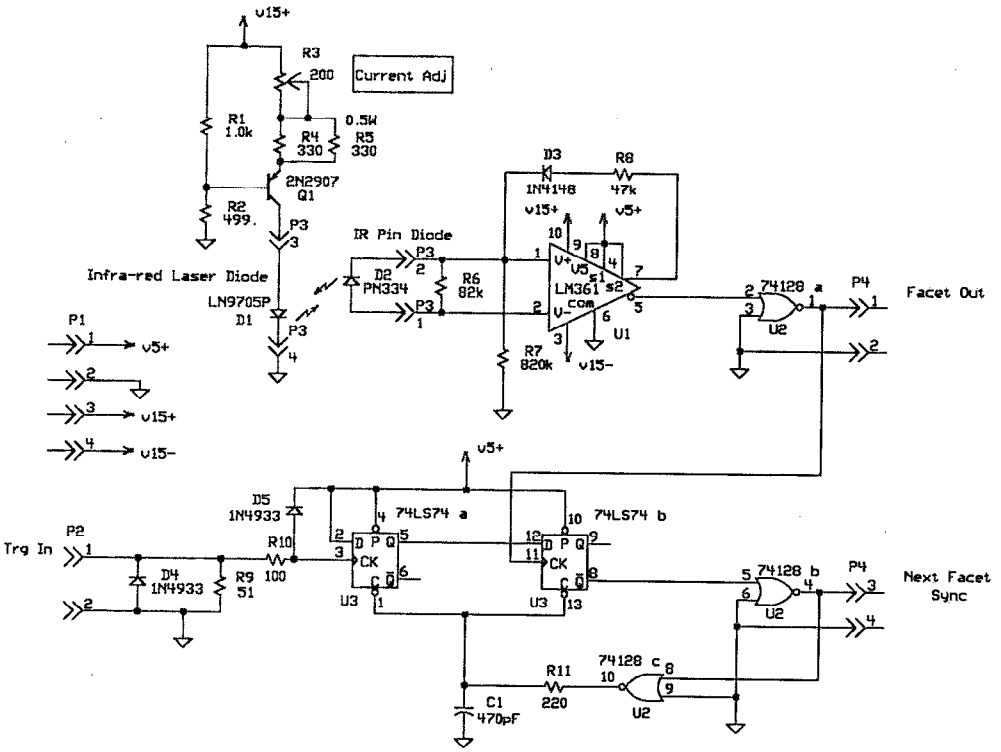

FIG. 2. Circuit for the rotating mirror facet detector.

the right flip-flop occurs simultaneously with a rising edge of the rectangular wave from the comparator. Thus, the digitizers are always triggered at the same point in the rotation of a facet, while the manual trigger allows the data-taking sequence to begin in the next period of the rectangular wave form.

E. Photodiode electronics

The detector comprises two 16-element linear photodiode arrays (UDT, model MOD171-1) laid end to end for a total length of 5.08 cm. This photodiode array can be operated in the photoconductive mode, but in this experiment a large back bias was not used. Each photodiode element is 0.157 cm wide and 0.122 cm high (the longer dimension running perpendicular to the length of the array). The projected image of the photodiode element onto the object plane is therefore 0.068 cm wide compared to the 15 cm width of the entire field of view, and the uncertainty in position due to the finite photodiode element size is 0.45% of the field of view.

The current-to-voltage converter circuit used with each photodiode is shown in Fig. 3. An NE5539 high-speed video op amp converts the photocurrent to a voltage, and the LH0002 line driver is used to send this signal to the digitizers over 50 Ω coaxial cable a few meters in length. The power supply voltage V_{CC} was chosen to restrict the noise component in the amplifier output to its minimum of 6 mV_{pp}. (In comparison, the resolution of the digitizers is 2.5 mV/bit).

The time response of the amplifier circuit was measured using a laser pulse from a Lambda Physik LPD 3001 dye laser. The excitation wavelength was at ~656 nm and the pulse width was 10 to 15 ns full-width at half maximum (FWHM). The laser pulse was attenuated to be comparable to the intensity of the arc used in our experiment. When the circuit is near saturation (~70% of the maximum output signal), it takes ~0.3 to 0.4 μs after the pulse for the amplifier output to return to zero level. (This is an extreme condition, and the time response is usually faster for smaller signals.) This translates to ~1% of the 41.7 μs frame period, or a ~1% uncertainty in position due to electronic time response alone. This is comparable to the uncertainty from the finite photodiode width, and the total uncertainty in the horizontal position is roughly the sum of these, or ~1.4% of the field of view. The digitizer sampling period should equal (or be less than) ~1.4% of a frame period in order to extract the maximum spatial information from the detector signal. Because of this, a digitizer sampling rate of 2.5 Ms/s (~100 samples per frame period) was used.

Another useful characterization of the photodiode system is that of the relative uniformity between channels. When the 32 photodiodes were illuminated with the same light intensity, the amplitude of the resulting channel outputs was found to vary by at most 8% from their median value. This level of channel to channel variability was sufficient for our application, which required only qualitative results. If quantitative measurements were desired, this variability in responsivity could be reduced through the use

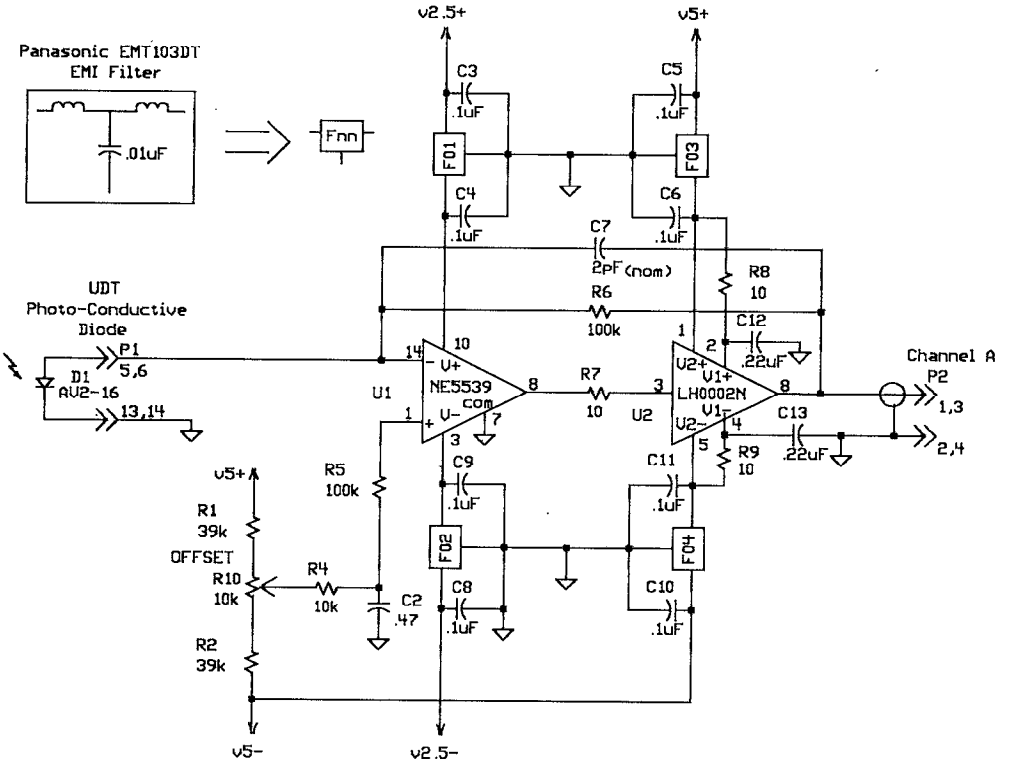

FIG. 3. Photodiode amplifier for one channel. Thirty-two separate channels are used in the camera.

of compensating components in the amplifiers, which would then be calibrated as required.

F. Camera sensitivity and dynamic range

The sensitivity of the camera is dependent on several factors, including the parameters of the optical configuration, frequency spectrum of the incident radiation, and photodiode/amplifier responsivity. In the calculations below, the spectral dependence of the photodiode responsivity has been neglected for simplicity, and a rough manufacturer's-specified nominal value of 0.3 A/W (in the visible light regime) has been employed. Note that, with our parameters, the mirror facet acts as the entrance pupil for the optical system, due to its small size, and restricts the amount of light reaching the detector from any point on the object. Thus, all of the light rays which arrive at the mirror facet will, in fact, travel through the remaining optics and into the detector. The amount of light which is incident on the detector is proportional to the solid angle subtended by the mirror facet (measured from the object), the surface radiance of the object, the inverse of the net optical magnification, and the area of the detector. Incorporating these factors with the photodiode response and amplifier gain, the resulting camera responsivity is 6 $\mathrm{mV/W\,cm^{-2}\,sr^{-1}}$). This value is defined as the ratio between photodiode amplifier output voltage and the input radiation, which is characterized by the surface radiance of the imaged object per solid angle in the direction of the mirror facet ($\mathrm{W\,cm^{-2}\,sr^{-1}}$).

The camera responsivity combined with the noise level determines the radiance detection threshold, i.e., the minimum radiance that can be detected above the 3 mV amplitude noise. The detection threshold, which is a measure of camera sensitivity, is therefore 0.3 $\mathrm{W\,cm^{-2}\,sr^{-1}}$ at the amplifier outputs. Additionally, a simple calculation involving the maximum output voltage amplitude of 1.7 V in our circuit yields an amplifier dynamic range of 55 dB.

The camera as described has low sensitivity, appropriate for our high light intensity application. Increased sensitivity could be obtained using other detector systems, such as photomultipliers, or alternative optical arrangements, e.g., with the addition of a third lens between the rotating mirror and the object. In fact, a considerable increase in sensitivity (orders of magnitude) should be achievable in this manner.

G. Digitization and software

The voltage levels from the photodiode amplifiers were digitized using a set of eight four-channel 8 bit Aeon Systems model 3248 digitizers. Each channel was equipped with 32 kilobytes of memory in order to store the results of a movie. The sampling clock rate, which is user programmable, was set to 2.5 MHz in our experiment, resulting in a frame width of 104 samples. This allowed a total of 314 frames of images to be stored in digitizer memory after triggering, each frame consisting of a grid of 32×104 points.

After the data was acquired, images could be conveniently transferred from digitizer memory to an IBM com-

patible 386 personal computer for display. The software developed to accomplish this was written in the Microsoft QuickBasic programming language, along with a few assembly language subroutines to facilitate the transfer of the large amounts of data involved. In order to access any particular frame of image data, the digitizer memory address offset was calculated, and the appropriate block of memory from the transient digitizers was then transferred. Due to small variations between channels in the base line signal from each photodiode–amplifier pair, the calibrated black-level values of each channel were subtracted from the data to obtain a measure of the true arc luminosity signal.

With the image data in computer memory, the picture could then be displayed on a high resolution VGA screen, in 8 bit gray scale or using a false color mapping scheme. In addition to simple playback of the movie, provisions were also made to advance through the movie, viewing frame by frame, in forward or reverse, allowing detailed examination of the images. Movies could be saved onto disk, so that they could be viewed in the future. Stand-alone movies (needing no software support) were also made which could be distributed on diskettes to other parties.

III. SAMPLE IMAGES OF A MODEL FURNACE ARC

This section displays excerpts from movies or an unstable arc. The experimental apparatus is discussed in Ref. 6, but a few comments are included here to assist the reader. In this experiment a 15 kV pulse is momentarily applied between a conical cathode and planar anode to break down an intervening 0.5 cm gap in air. A few microseconds later a large capacitor bank at lower voltage is discharged through the initial arc and sustains it for a few milliseconds. The camera is synchronized to begin recording at the high voltage pulse. The outline of the cathode, the anode, and a tungsten plug protruding up from the center of the anode are superimposed on each of the frames of Fig. 4 after processing the data.

The arc current returns through vertical rods (not shown in frames) to the right of the cathode. The magnetic field from this return current initially drives the arc to the left, and this initial displacement is then overcome by a kink instability that quickly extends the loop of plasma to the left. This is illustrated by the frame sequence in Fig. 4: in frame 1 the gap has just broken down, in frame 8 (292 μs later) the arc has moved to the left edge of the tungsten plug, and by frame 32 (1 292 μs after breakdown) the arc has become quite distended. Between frames 34 and 35 the arc is interrupted and restrikes closer to the center of the gap. The new arc can be seen moving to the left in frame 35. The restrike and "blow out" sequence is repeated in frames 35 to 41, and again in frames 41 to 47.

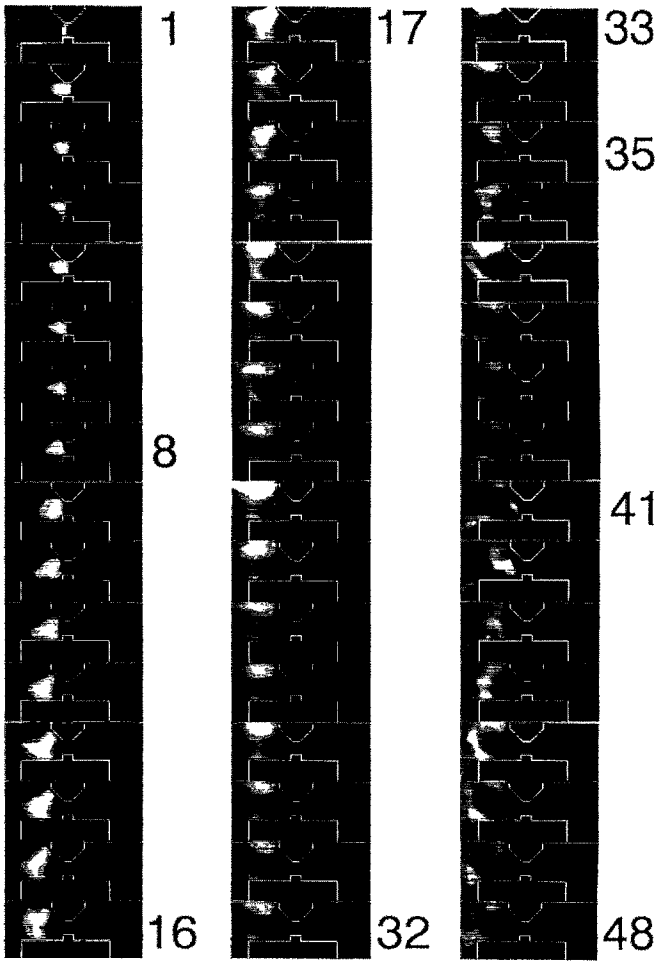

FIG. 4. Excerpt from a movie of an unstable arc showing "blow out" (frames 9–34) and several restrikes (frames 35, 41, and 47). The superimposed lines indicate the location of the cathode (top) and anode (bottom). The time interval between frames is 41.7 μs, and the frame sequence progresses from top to bottom in each column and begins with the left column. Frame numbers are indicated for a few key frames.

IV. DISCUSSION

The description of the camera operation makes it clear that different vertical bands in a frame are not captured at the same moment in time. Thus although the framing rate is 24 000 frames/s, motion across the field of view in a time interval comparable to the interframe period will result in some blurring of the image. When viewing a single frame, this effect must be kept in mind. But the usefulness of any camera is determined by the accuracy required by the user, and if the phenomenon observed changes sufficiently slowly that blurring is slight and tolerable, then the advantages of immediate retrieval, low cost, and ease of operation make this camera an attractive diagnostic.

Another useful feature of this camera design is its pretrigger capability (similar to that on a digital oscilloscope) which can be used for capturing random events where there is no external trigger. The event itself can act as the trigger and, if the digitizers are used in a free-run mode, precursors of the event will be recorded.

ACKNOWLEDGMENTS

The authors would like to thank F. Cosso for his assistance with the trigger and preamp electronics. This work was supported by NSF Grant No. ECS-8814184.

[1] L. L. Endelman, ISPRS J. Photogrammetry Remote Sensing **46**, 249 (1991).
[2] H. L. Walmsley, G. R. Jones, F. Haji, and D. C. Strachan, J. Phys. D **10**, 383 (1977).
[3] Klaus P. Nachtigall and Juergen Mentel, IEEE Trans. Plasma Sci. **19**, 947 (1991).
[4] B. Bowman, G. R. Jordan, and F. Fitzgerald, J. Iron Steel Inst., June 798 (1969).
[5] G. R. Jordan, B. Bowman, and D. Wakelam, J. Phys. D **3**, 1089 (1970).
[6] P. M. Bellan and J. W. Higley, IEEE Trans. Plasma Sci. **20**, 1026 (1992).
[7] US patent applied for.